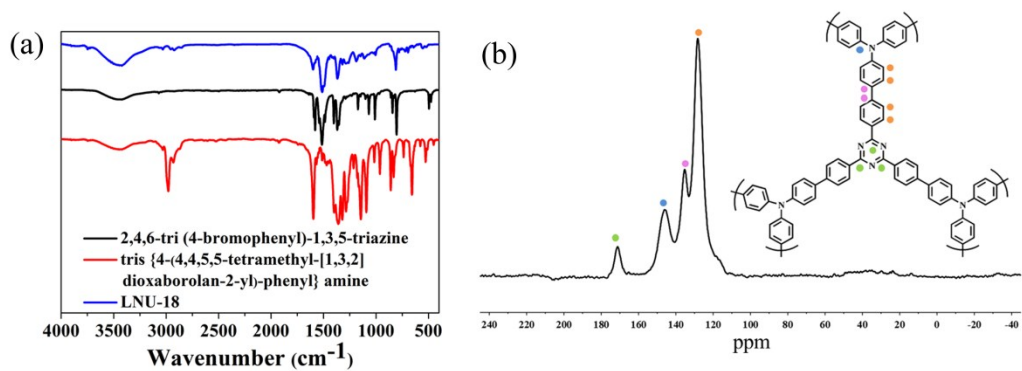


*Supporting Information*

**Carbonized porous aromatic framework to achieve customized nitrogen atoms for enhanced supercapacitor performance**

*Yunbo Zhao,<sup>a</sup> Naishun Bu,<sup>b</sup> Huimin Shao,<sup>a</sup> Qian Zhang,<sup>a</sup> Bin Feng,<sup>a</sup> Yanmei Xu,<sup>a</sup> Guiyue Zheng,<sup>a</sup> Ye Yuan,<sup>c</sup> Zhuojun Yan<sup>\*a</sup> and Lixin Xia<sup>\*a</sup>*

- a. College of Chemistry, Liaoning University, Shenyang 110036, P. R. China.  
E-mail: zjyan@lnu.edu.cn; lixinlia@lnu.edu.cn
- b. School of Environmental Science, Liaoning University, Shenyang 110036, P. R. China.
- c. Key Laboratory of Polyoxometalate Science of the Ministry of Education, Faculty of Chemistry, Northeast Normal University, Changchun 130024, P. R. China.



**Fig. S1** (a) FTIR and (b) solid-state  $^{13}\text{C}$  CP/MAS NMR spectra for LNU-18.

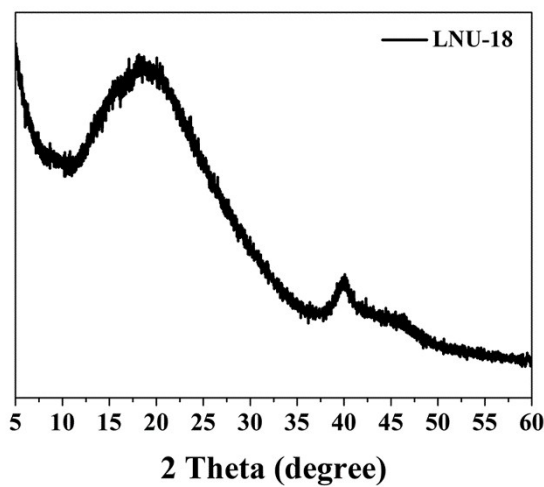


**Fig. S2** PXRD pattern for LNU-18.

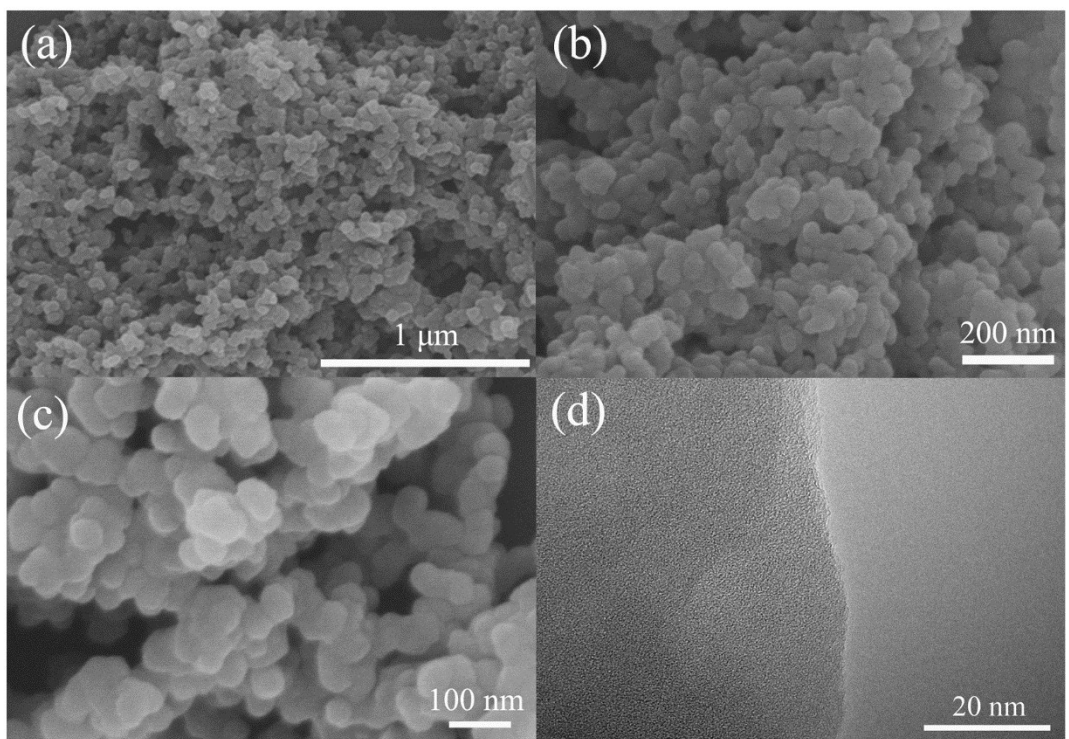


**Fig. S3** (a, b, c) SEM micrographs for LNU-18; (d) TEM micrograph for LNU-18.

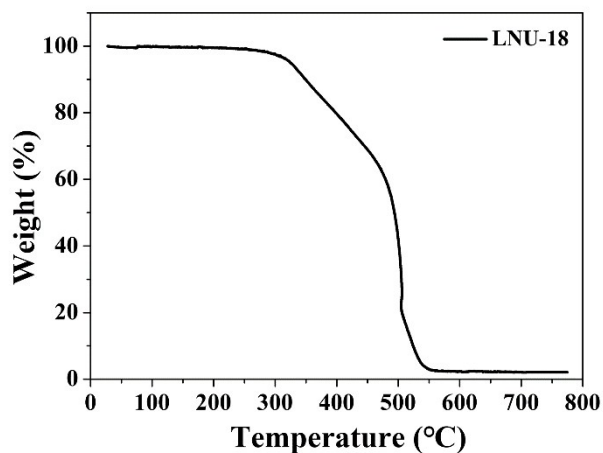


**Fig. S4** TGA curve for LNU-18 in air condition.

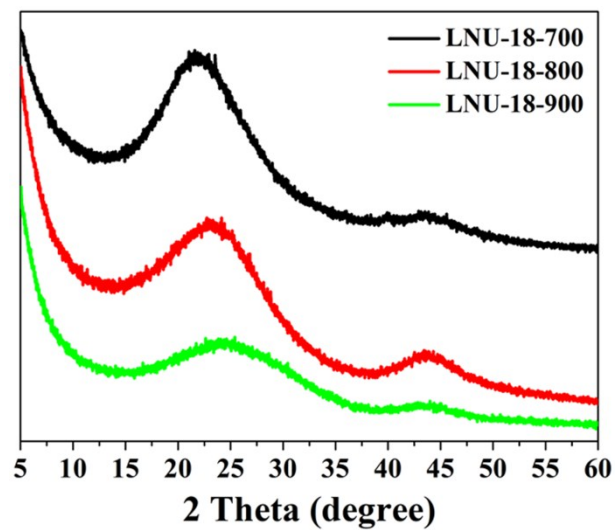


**Fig. S5** PXRD patterns for LNU-18-700, LNU-18-800, and LNU-18-900.

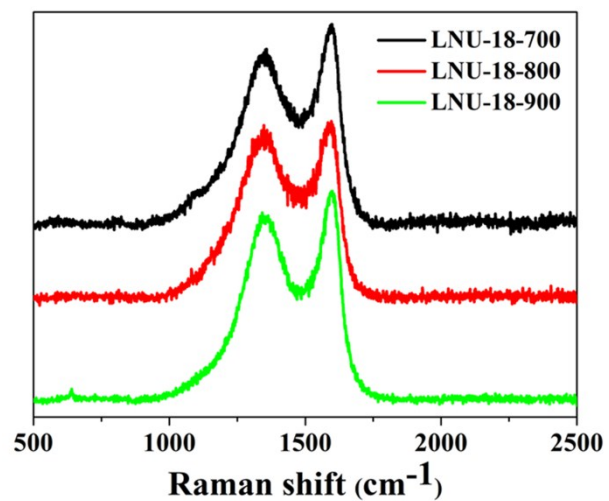


**Fig. S6** Raman spectra for LNU-18-700, LNU-18-800, and LNU-18-900.

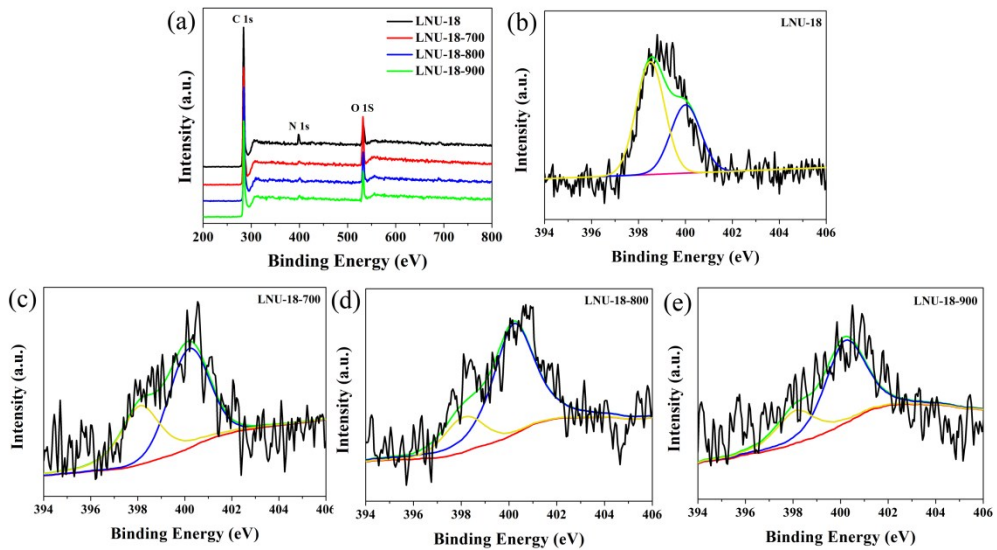


**Fig. S7** (a) XPS spectra for LNU materials; N 1s XPS for (b) LNU-18, (c) LNU-18-700, (d) LNU-18-800, and (e) LNU-18-900.

**Table S1** Elemental compositions of C, N and O, and relation contents of nitrogen species to N 1s

Samples	C (at.%)	N (at.%)	O (at.%)	N <sub>pyrrolic</sub> (%)	N <sub>triazine</sub> (%)
LNU-18-700	84.53	1.73	13.74	67.95	32.05
LNU-18-800	85.65	3.06	11.29	81.88	18.12
LNU-18-900	86.46	2.04	11.51	74.20	25.80

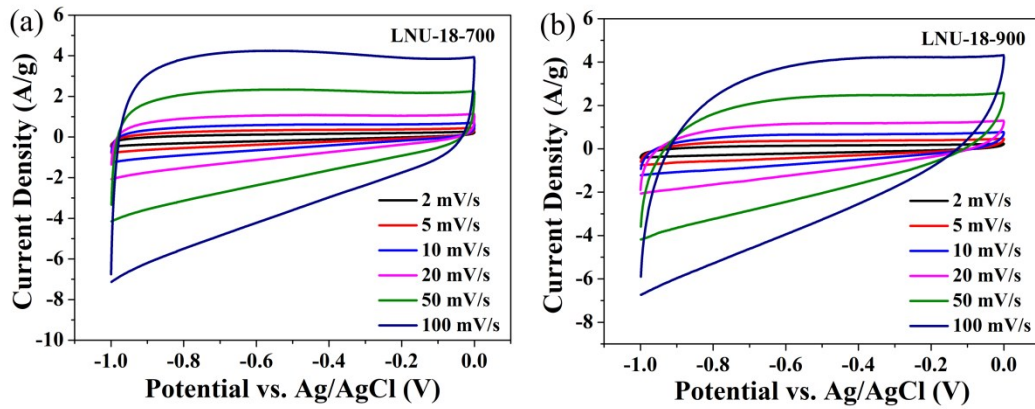


**Fig. S8** CV curves for (a) LNU-18-700 and (b) LNU-18-900 at different scan rates.

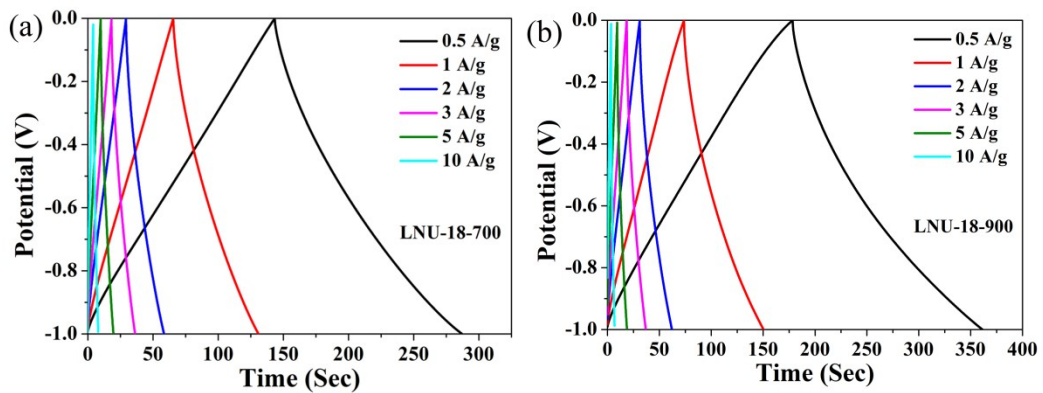


**Fig. S9** GCD curves for (a) LNU-18-700 and (b) LNU-18-900 at different current densities.

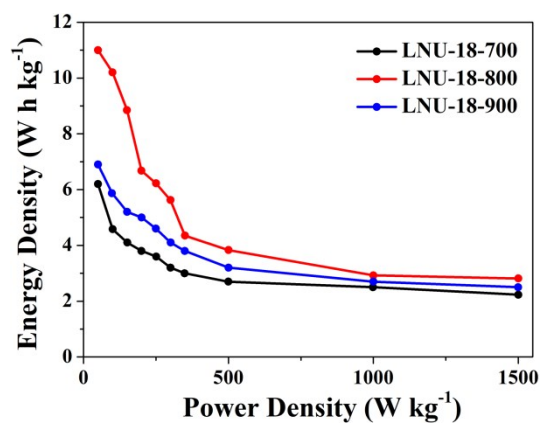


**Fig. S10** Ragone plots for LNU-18-700, LNU-18-800, and LNU-18-900.

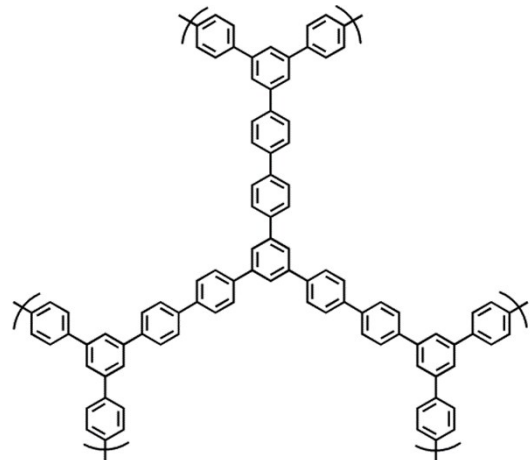


**Fig. S11** The structure for PAF-48.

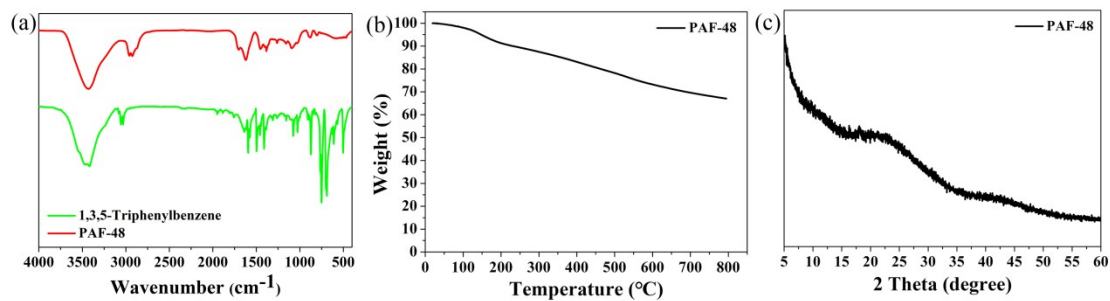


**Fig. S12** (a) FTIR spectra for PAF-48; (b) TGA curve for PAF-48 in  $\text{N}_2$  condition; (c) PXRD pattern for LNU-18.

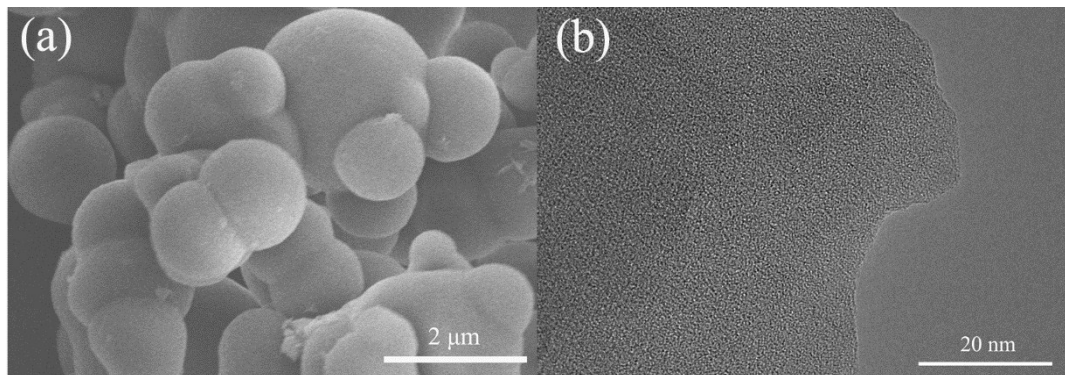


**Fig. S13** (a) SEM and (b) TEM micrograph for PAF-48.

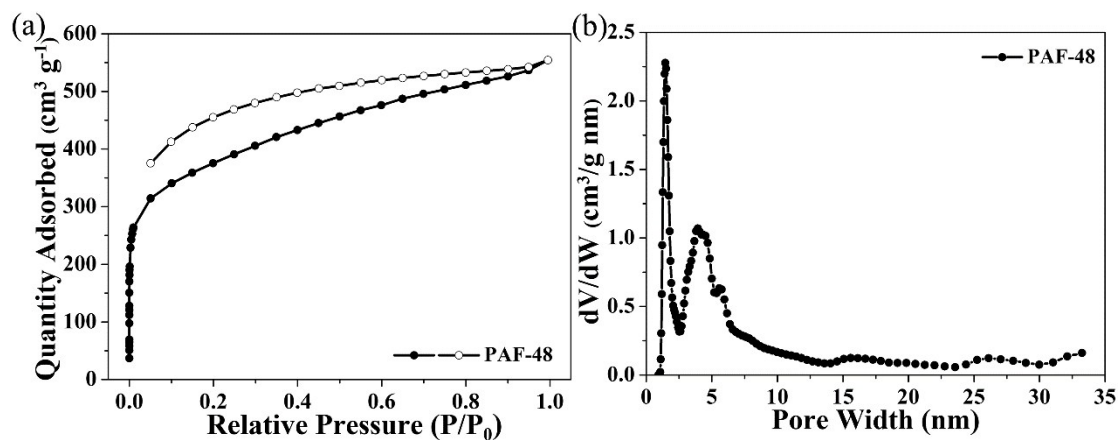


**Fig. S14** (a) Nitrogen adsorption (closed)/desorption (open) isotherms for PAF-48; (b) Pore size distribution curve for PAF-48 calculated by the NLDFT method.

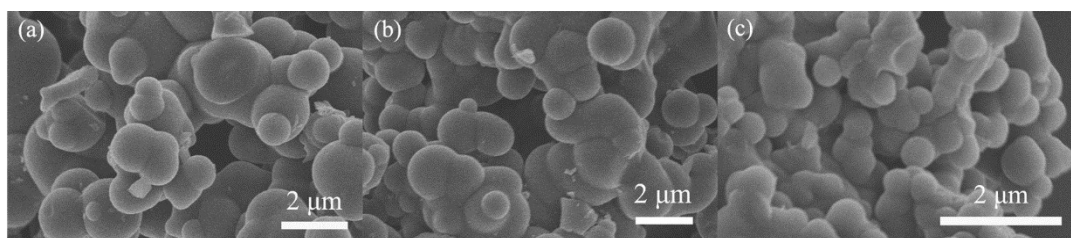


**Fig. S15** SEM micrographs for PAF-48-700 (a), PAF-48-800 (b) and PAF-48-900 (c).

**Table S2** Specific capacitance (F/g) of the samples at different current densities

precursor	PAF-48			LNU-18		
carbon materials	PAF-48-700	PAF-48-800	PAF-48-900	LNU-18-700	LNU-18-800	LNU-18-900
0.5 A/g	125	54	52	72	269	92
1 A/g	60	46	39	65	237	77
2 A/g	41	40	28	58	211	62
3 A/g	36	37	23	54	195	55
5 A/g	31	33	20	49	169	47
10 A/g	26	28	17	39	126	34

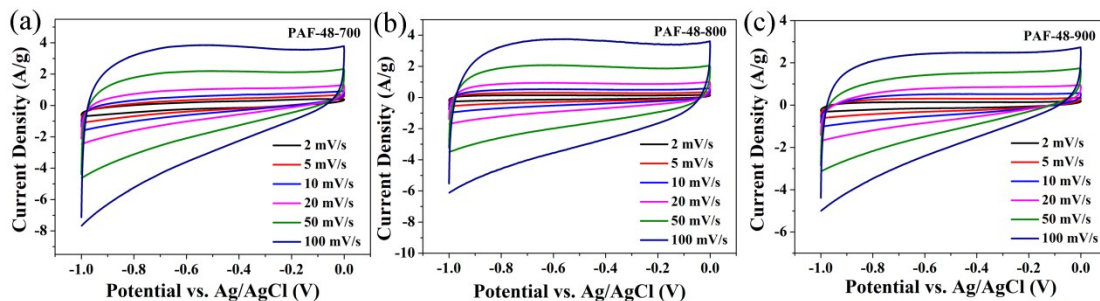


**Fig. S16** CV curves for (a) PAF-48-700, (b) PAF-48-800, and (c) PAF-48-900 at different scan rates.

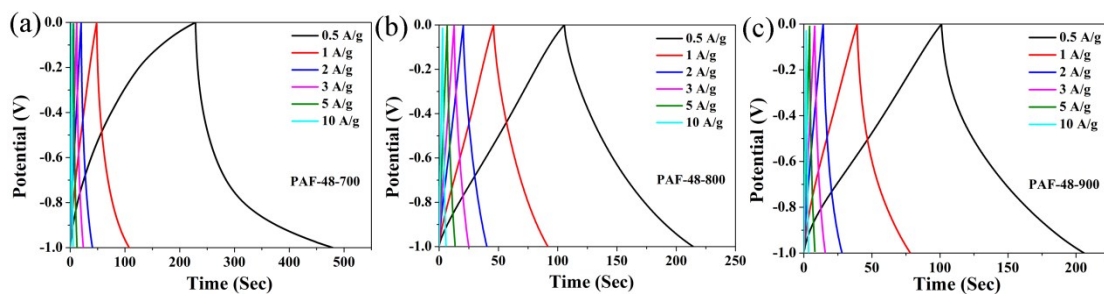


**Fig. S17** GCD curves for (a) PAF-48-700, (b) PAF-48-800, and (c) PAF-48-900 at different current densities.

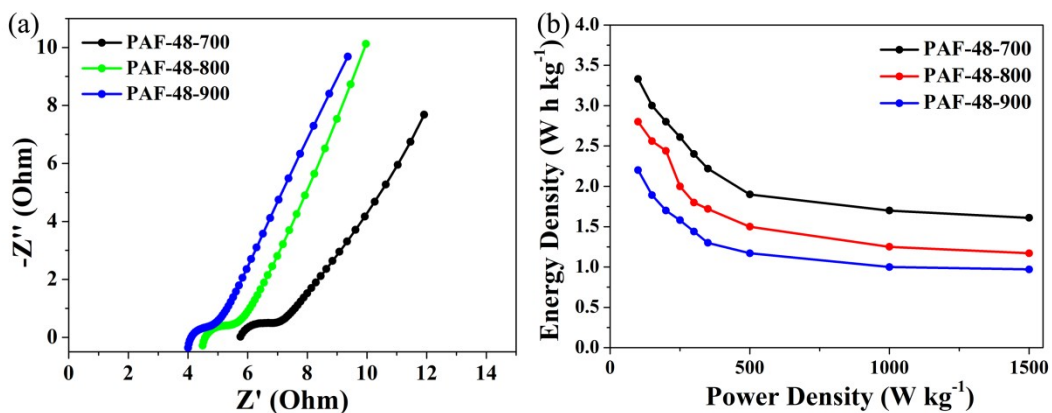


**Fig. S18** (a) Nyquist plots for PAF-48s in the frequency range from 0.01 Hz to 100 kHz in the three-electrode system; (b) Ragone plots for PAF-48s in the two-electrode system.

**Table S3** Comparison of specific capacitance data of previous reported carbon materials

Sample	Capacitance (F/g)	Current density (A/g)	Electrolyte	Reference s
<b>RGHs-1</b>	230.4	0.3	6 M KOH	1
<b>CS-OH</b>	167	1	1 M H <sub>2</sub> SO <sub>4</sub>	2
<b>IMPC</b>	258	0.5	1 M H <sub>2</sub> SO <sub>4</sub>	3
<b>NPHCMs-65-700</b>	208	0.5	6 M KOH	4
<b>NCS</b>	203	0.5	6 M KOH	5
<b>TpPa-COF@PANI</b>	95	0.2	1 M H <sub>2</sub> SO <sub>4</sub>	6
<b>NWNU-COF-1</b>	155.38	0.25	6 M KOH	7
<b>ACOF1</b>	234	1	6 M KOH	8
<b>C-800</b>	228	1	6 M KOH	9
<b>c-CBAP-N</b>	203.2	1	6 M KOH	10
<b>TAT-CMP-2</b>	183	1	1 M Na <sub>2</sub> SO <sub>4</sub>	11
<b>N3-CMP</b>	260	0.1	1 M Na <sub>2</sub> SO <sub>4</sub>	12

## References

- [1] M. Jiang, J. L. Zhang, F. Qiao, R. Y. Zhang, L. B. Xing, J. Zhou, H. Y. Cui and S. P. Zhuo, *RSC Adv.*, 2016, **6**, 48276-48282.
- [2] X. Tong, H. Zhuo, S. Wang, L. X. Zhong, Y. J. Hu, X. W. Peng, W. J. Zhou and R. C. Sun, *RSC Adv.*, 2016, **6**, 34261-34270.
- [3] D. Puthusseri, V. Aravindan, S. Madhavi and S. Ogale, *Energy Environ. Sci.*, 2014, **7**, 728-735.
- [4] N. Zhang, F. Liu, S. D. Xu, F. Y. Wang, Q. Yu and L. Liu, *J. Mater. Chem. A*, 2017, **5**, 22631-22640.
- [5] Y. L. Wang, S. Y. Dong, X. Q. Wu, X. W. Liu and M. G. Li, *J. Mater. Sci.*, 2017, **52**, 9673-9682.
- [6] S. Liu, L. Yao, Y. Lu, X. L. Hua, J. Q. Liu, Z. Yang, H. Wei and Y. Y. Mai, *Mater. Lett.*, 2019, **236**, 354-357.
- [7] R. Xue, H. Guo, L. G. Yue, T. Wang, M. Y. Wang, Q. Li, H. Liu and W. Yang, *New J. Chem.*, 2018, **42**, 13726-13731.
- [8] G. Kim, J. Yang, N. Nakashima and T. Shiraki, *Chem. Eur. J.*, 2017, **23**, 17504-17510.
- [9] M. Kim, P. Puthiaraj, Y. J. Qian, Y. Kim, S. Jang, S. Hwang, E. Na, W. Ahn and S. Shim, *Electrochim. Acta*,

**2018**, **284**, 98-107.

- [10] M. Kim, P. Puthiaraj, J. So, H. Seong, J. Ryu, W. Ahn and S. Shim, *Synth. Met.*, 2018, **243**, 115-120.
- [11] X. C. Li, Y. Z. Zhang, C. Y. Wang, Y. Wan, W. Y. Lai, H. Pang and W. Huang, *Chem. Sci.*, 2017, **8**, 2959-2965.
- [12] J. M. Lee, T. H. Wu, B. M. Alston, M. E. Briggs, T. Hasell, C. C. Hu and A. I. Cooper, *J. Mater. Chem. A*, 2016, **4**, 7665-7673.